



A Direct Cortico-Nigral Pathway as Revealed by Constrained Spherical Deconvolution Tractography in Humans

Alberto Cacciola^{1*}, Demetrio Milardi^{1,2}, Giuseppe P. Anastasi¹, Gianpaolo A. Basile¹, Pietro Ciolli¹, Mariangela Irrera¹, Giuseppina Cutroneo¹, Daniele Bruschetta¹, Giuseppina Rizzo¹, Stefania Mondello¹, Placido Bramanti² and Angelo Quartarone^{1,2}

¹ Department of Biomedical, Dental Sciences and Morphological and Functional Images, University of Messina, Messina, Italy, ² IRCCS Centro Neurolesi "Bonino Pulejo," Messina, Italy

OPEN ACCESS

Edited by:

Bogdan Draganski,
University of Lausanne, Switzerland

Reviewed by:

Laurent Petit,
Centre National de la Recherche
Scientifique, France
Christian Lambert,
University of London, UK

*Correspondence:

Alberto Cacciola
alberto.cacciola0@gmail.com

Received: 28 December 2015

Accepted: 11 July 2016

Published: 26 July 2016

Citation:

Cacciola A, Milardi D, Anastasi GP, Basile GA, Ciolli P, Irrera M, Cutroneo G, Bruschetta D, Rizzo G, Mondello S, Bramanti P and Quartarone A (2016) A Direct Cortico-Nigral Pathway as Revealed by Constrained Spherical Deconvolution Tractography in Humans.
Front. Hum. Neurosci. 10:374.
doi: 10.3389/fnhum.2016.00374

Substantia nigra is an important neuronal structure, located in the ventral midbrain, that exerts a regulatory function within the basal ganglia circuitry through the nigro-striatal pathway. Although its subcortical connections are relatively well-known in human brain, little is known about its cortical connections. The existence of a direct cortico-nigral pathway has been demonstrated in rodents and primates but only hypothesized in humans. In this study, we aimed at evaluating cortical connections of substantia nigra *in vivo* in human brain by using probabilistic constrained spherical deconvolution (CSD) tractography on magnetic resonance diffusion weighted imaging data. We found that substantia nigra is connected with cerebral cortex as a whole, with the most representative connections involving prefrontal cortex, precentral and postcentral gyri and superior parietal lobule. These results may be relevant for the comprehension of the pathophysiology of several neurological disorders involving substantia nigra, such as parkinson's disease, schizophrenia, and pathological addictions.

Keywords: substantia nigra, CSD, basal ganglia, tractography, connectivity, cortex, parkinson disease

INTRODUCTION

Substantia Nigra (SN) is a neuronal structure located in the ventral part of the midbrain, between crus cerebri and tegmentum. The postero-medial region of SN, known as "pars compacta" (SNc), is one of the four primary dopaminergic nuclei of the brain, together with the ventral tegmental area (VTA), the retrorubral area and the arcuate nucleus of hypothalamus (Nestler et al., 2009), and it is mainly connected with the dorsal striatum through the nigro-striatal pathway (Voorn et al., 2004). The antero-lateral zone, the "pars reticulata" (SNr), consists of GABAergic neurons which receive afferents from the striatum and subthalamic nucleus (STN) and in turn project to ventral-anterior (VA) and ventral-lateral (VL) thalamic nuclei (Zhou and Lee, 2011).

It is well-known that SN exerts a regulatory function on the basal ganglia circuitry (Guatteo et al., 2009), and it is involved in several neurological and neuropsychiatric disorders, such as Parkinson's Disease (Carman, 1968), schizophrenia (Weinberger, 1987), and pathological addictions (Wise, 2009).

Although several reports have demonstrated the existence of an extensive sub-cortical network for both SNc and SNr (Düzel et al., 2009; Menke et al., 2010; Chowdhury et al., 2013), less is known about the existence of direct cortico-nigral connections in the human brain.

The existence of a direct cortico-nigral pathway was postulated for the first time by Foix and Niculescu (1925) and then re-proposed by Rinvik and co-workers, who suggested the presence of direct projections arising from premotor area and reaching SN (Rinvik, 1966).

However, it was only the 1974 when direct cortico-nigral connectivity was demonstrated in cats by means of fiber degeneration methods (Fink-Heimer staining) (Afifi et al., 1974). On the contrary some studies in primates failed to reveal representative direct connections between cortex and ventral midbrain, resulting only in sparse or isolated fiber tracts (Leichnetz and Astruc, 1976; Künzle, 1978; von Monakow et al., 1979).

Further investigations in rodents revealed cortico-nigral connections between prefrontal cortex (PFC) and SN, using antero- and retrograde fiber tracers (Bunney and Aghajanian, 1976; Beckstead, 1979; Sesack et al., 1989; Naito and Kita, 1994; Jasmin et al., 2004; Zakiewicz et al., 2014; Höglinger et al., 2015) and ablation techniques (Carter, 1982; Kornhuber, 1984).

In addition, in an auto radiographic tracing study, it was found that area 6 in the raccoon projected to the ipsilateral SNc (Sakai, 1978).

Finally, in a more recent study on macaca monkeys, Frankle et al. (2006) injected anterograde tracers into the orbital (OFC), cingulate and dorsolateral prefrontal (dlPFC) cortices, demonstrating direct connections from OFC and dlPFC to SN, whilst cingulate cortex was mainly connected to VTA (Frankle et al., 2006).

On the one hand, even if tract-tracing methods are the gold standard for studying the anatomo-physiology of basal ganglia, on the other hand, they still remain highly invasive techniques and therefore they cannot be used to study human brain *in vivo* (McFarland and Haber, 2000; Nambu et al., 2000; Kita, 2001).

However, in recent years, a growing interest in neuroimaging studies and several developments in magnetic resonance imaging have permitted to shed new light on the whole brain connectivity.

In this regard, Diffusion Tensor Imaging (DTI) is a modeling technique which allows, from the analysis of anisotropic water motion in white matter, the non-invasive reconstruction, and visualization of white matter fiber bundles (Mormina et al., 2015); it thus permits to estimate connectivity patterns between distinct brain regions (Basser et al., 1994; Henderson, 2012; Le Bihan and Johansen-Berg, 2012). Tractographic findings strongly depend on the diffusion model adopted: indeed, it is known that DTI suffers from several limitations such as large reconstruction biases and less reliability for fibers with complex configuration (e.g., crossing, fanning, kinking fibers; Parker and Alexander, 2005; Behrens et al., 2007; Jones and Cercignani, 2010; Farquharson et al., 2013). Consequently, several sequences and related signal modeling have been recently developed and used for exploring neural connectivity in normal subjects (Parker and Alexander, 2005; Jbabdi and Johansen-Berg, 2011; Farquharson et al., 2013; Jang et al., 2013; Jbabdi et al., 2015).

In particular, constrained spherical deconvolution (CSD) is able to reduce reconstruction biases and to provide more robust data, estimating one or more fiber orientations in presence

of intravoxel orientational heterogeneity (Tournier et al., 2007, 2008; Farquharson et al., 2013; Milardi et al., 2016b).

To date, only few multitensorial DTI studies have focused on the connectivity of SN in human subjects (Menke et al., 2010; Chowdhury et al., 2013). In particular, Menke et al. used probabilistic DTI tractography with the aim of differentiating SNc and SNr according to their different connectivity profile. They demonstrated that these regions are both likely connected to cerebral cortex by means of the thalamus. SNc showed higher connectivity profile with prefrontal cortex, whilst SNr was more connected with motor and premotor cortices (Menke et al., 2010). Chowdhury et al. investigated the well-characterized anatomical projections between the SN/VTA and striatum, providing a new method for subdividing the SN/VTA based on connectivity to the striatum (Chowdhury et al., 2013). Furthermore, they claimed that “direct projections between the SN/VTA and other structures exist, for example with the prefrontal cortex (Künzle, 1978).”

Finally, Kwon and Jang (2014) directly aimed the question of different patterns of connectivity between SN/VTA, showing that SN is connected with several brain structures such as corpus callosum, primary sensory cortex, premotor cortex, caudate nucleus, putamen, nucleus accumbens, temporal-occipital lobes, pontine basis, anterior lobe of cerebellum, external capsule (Kwon and Jang, 2014).

Challenging the classical view of the basal ganglia network based on the “direct,” “indirect” (Leblois et al., 2006), and “hyperdirect” pathways (Nambu et al., 1996, 2002), we have recently demonstrated the existence of a possible cortico-pallidal connectivity in humans (Milardi et al., 2015; Smith and Wichmann, 2015), which was then corroborated by a magnetoencephalography-local field potentials study in dystonic patients (Neumann et al., 2015). Furthermore, this hypothesis would meet the vision that the cortico-basal ganglia network consists of several, parallel, segregated, and functionally distinct, but homologous loop.

In this framework, we supported the hypothesis that the SN is not only a part of the subcortical basal ganglia network, but it is also connected with cortex, by means of an additional, parallel circuit. In the present study we provided tractographic findings of the existence of a cortico-nigral pathway in humans, confirming the previously existing literature based on animal studies.

MATERIALS AND METHODS

Participants

We recruited a total of 15 human subjects (male: 8, female: 7; average age 35.46 ± 11 years) with no previous history any overt neurological, physical or psychiatric disease. The research followed the tenets of the Declaration of Helsinki; written informed consent was signed from all included subjects, after explanation of the nature and possible consequences of the procedure. The study was approved by the institutional review board of IRCCS Bonino Pulejo, Messina, Italy (Scientific Institute for Research, Hospitalization and Health Care), protocol number 15/2012.

Data Acquisition

The study was performed with a 3T Achieva Philips scanner using a 32-channels SENSE head coil. In each patient a structural 3D high-resolution T1 weighted Fast Field Echo (FFE) sequence was acquired using the following parameters: repetition time 25 ms; echo time 4.6 ms; flip angle 30°; FOV 240 × 240 mm²; reconstruction matrix 240 × 240; voxel size 1 × 1 × 1 mm; slice thickness 1 mm. The acquisition time was 6 min. Furthermore, a 3-D high resolution T2 weighted Turbo Spin Echo (TSE) sequence was obtained using the following parameters: repetition time 2500 ms; echo time 380 ms; FOV 250 × 250 mm²; reconstruction matrix 312 × 312; voxel size 0.8 × 0.8 × 0.8 mm; slice thickness 0.8 mm, The acquisition time was 9 min and 38 s.

The use of 3D TSE sequence allowed obtaining high-resolution images with a relative short acquisition time. At same time this sequence permitted to obtain a fine representation of the iron loaded nuclei due to T2* effect linked with the use of a very long echo-time (**Figure 1**).

Furthermore, a DWI dataset was obtained with a dual phase encoded pulsed gradient spin echo sequence (Embleton et al., 2010); following parameters were adopted: *b*-value 1500 s/mm², 61 gradient diffusion directions evenly distributed on a sphere more 3 un-weighted b0 volumes, echo-time 54 ms, repetition time 11,884 ms, FOV 240 × 240 mm² resulting in isotropic 2 mm voxel resolution.

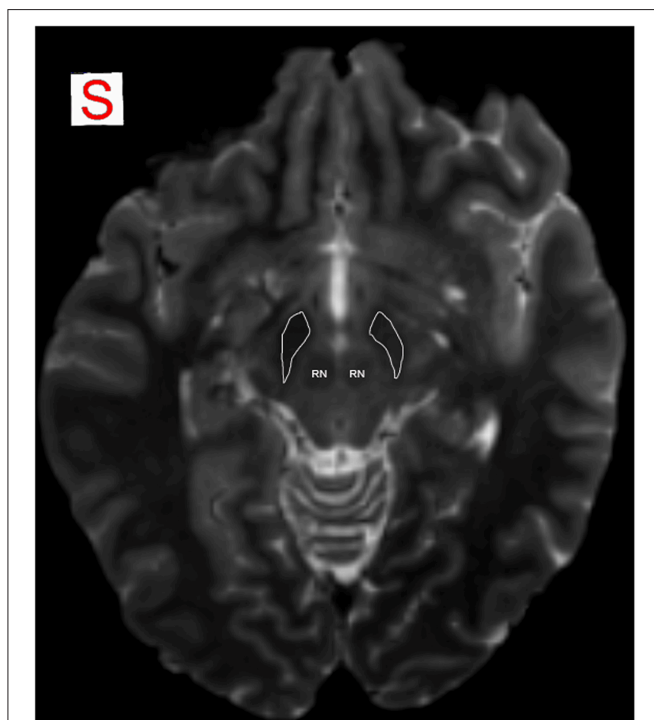


FIGURE 1 | MRI identification of SN. SN is detectable as an hypointense region in axial plane in T2-weighted images, due to T2* effect that allows a better visualization of the iron-loaded nuclei. Anatomical relations of SN with RN are well identifiable. RN, red nucleus; SN is encircled in white.

DWI Pre-processing and Co-registration

All diffusion images were corrected for motion as well as for Eddy Currents distortion artifacts using tools available within SPM8 MATLAB tool (<http://www.fil.ion.ucl.ac.uk/spm/software/spm8/>) and FSL. In brief, affine transformation based on b0 volumes was estimated and applied to diffusion images using Diffusion tool (<https://sourceforge.net/projects/spmtools/>); a displacement field map was created using topup FSL function on the basis of two b0 images acquired in opposite phase encoding directions. Such displacement field map was eventually fed to diffusion dataset using Unwarp and Fieldmap SPM8 toolboxes (<http://www.fil.ion.ucl.ac.uk/spm/toolbox/unwarp/>). Rotational parts of transformations were applied to individual gradient directions. High Resolution T1 and T2 images were then co-registered to preprocessed DWIs using a pipeline outlined in (Besson et al., 2014): in particular, Cerebral Spinal Fluid (CSF) masks were estimated from average of b0 images as well as from T1 ones using New Segment SPM8 utility. Then, CSFs of structural scans were warped to match CSF estimated from b0-image using FLIRT and FNIRT FSL utilities (<http://fsl.fmrib.ox.ac.uk/fsl/fslwiki/>). Deformation fields were eventually applied to T1s to obtain an alignment as accurate as possible between structural and diffusion data.

This workflow led to much better cortical and subcortical correspondence than traditional affine co-registrations involving T1 and DWIs. In this way, we minimized possible misalignment biases coming from usage, in diffusion images space, of ROIs segmented in space of structural scans. This process is therefore fundamental to have an optimal anatomical correspondence, avoiding Regions of Interests (ROIs) to be slightly displaced and affected by CSF signal.

Segmentation of SN

The use of a very long echo-time in 3D T2-weighted TSE sequences allowed to obtain a reliable identification and segmentation of the iron loaded nuclei. In particular, by means of a viewer provided together with MRtrix package, the mask for SN was manually outlined by one of the authors bilaterally in T2-weighted images in the axial plane (**Figure 1**) superimposed on the color-coded FA map, where the SN typically appeared in green (Mori et al., 2004; Kwon and Jang, 2014). We localized the SN immediately above the pons, as a hypointense region between crus cerebri and tegmentum. Ascending in caudo-cranial direction, this region appeared to be expanded ventrally and we localized behind it the red nucleus (RN), in a more medial position. We were able to identify VTA as the medial hyperintense zone between RN and SN. In the upper sections of SN, we identified the STN as dorso-medial boundary and marked the SN in every ascending slices until the superior colliculi and the cerebral aqueduct disappeared. As posterior and anterior boundaries of the most superior section, the cerebral aqueduct and mammillary bodies were, respectively, delineated. STN becomes prominent in the axial plane including third ventricle, RN and the posterior commissure. The mask was better defined in both sagittal and coronal planes. It is worthy to note that the mask of SN was outlined small enough to avoid other white matter voxels and fiber streamlines in a neighboring area.

Cortical Parcellation

Cortical reconstruction and volumetric segmentation were performed on co-registered T1 images with the Freesurfer image analysis suite, which is documented and freely available for download online (<http://surfer.nmr.mgh.harvard.edu/>). Briefly, this processing involves motion correction and averaging (Reuter et al., 2010) of T1 weighted images, removal of non-brain tissue using a hybrid watershed/surface deformation procedure (Segonne et al., 2004), segmentation of the subcortical white matter and deep gray matter volumetric structures (Fischl et al., 2004), tessellation of the gray matter white matter boundary, automated topology correction (Ségonne et al., 2007), and surface deformation following intensity gradients to optimally place the gray/white and gray/cerebrospinal fluid borders at the location where the greatest shift in intensity defines the transition to the other tissue class (Fischl and Dale, 2000). Once the cortical models were completed, parcellation of the cerebral cortex into units with respect to gyral and sulcal structure (Desikan et al., 2006) was performed. Successively, the obtained parcellation and segmentation of each individual were visually inspected and, if needed, manually edited by one of the authors.

Tractography

To model diffusion signal, we used a modified High Angular Resolution Diffusion Imaging (HARDI) technique called non-negative CSD: this technique estimates the fiber Orientation Distribution Function (fODF) directly from deconvolution of DW signal with a reference single fiber response function (Tournier et al., 2007). Response function was estimated from the data on the basis of voxels having a Fractional Anisotropy index (FA) above 0.7, this threshold being a strong indicator that a single fiber population insists within those voxels. fODF estimation and tractography were performed using MRtrix software (<http://jdtournier.github.io/mrtrix-0.2/index.html>).

Using CSD to extract local fiber orientations we managed to overcome partial volume effects associated with DTI and also to improve, comparing with other types of HARDI acquisitions, the poor angular resolution achieved with QBI (Q-balls Imaging), while discarding DSI due to its longer acquisition time (Alexander and Barker, 2005; Tournier et al., 2008).

In our study, spherical harmonic degree was fixed equal to 8 in order to obtain robustness to noise. During tractographic reconstruction, tracking was stopped when one of the following conditions existed: step size = 0.2 mm, maximum angle = 10°, minimal fODF amplitude = 0.15. The latter parameter allowed to obtain more accurate reconstructions avoiding streamlines to enter GM in deep or passing through CSF; indeed, in those regions, estimated fODF amplitudes are lower than such cut-off. This is a more conservative choice with respect to usual standards, since we preferred to underestimate fiber bundles in order to have consistent reconstruction without false positive (Descoteaux et al., 2009; Tournier et al., 2011).

We performed, for each subject, probabilistic whole brain tractography by generating a total of one millions streamlines using WM masks both as seed and mask regions; before running tractography, we applied a small dilatation to WM masks in

order to allow streamlines to reach our ROIs, placed in GM, for subsequent analyses.

A further improvement in the definition of the fiber tracking was obtained by an anatomical model-based approach using regions of avoidance (ROAs) that, on the contrary, “filter out” the tracks (Verstynen et al., 2011). In particular, based on whole brain tractography, we have filtered out tracks by using SN as inclusion mask and basal ganglia as exclusion ones, isolating white matter reconstructed bundles traveling from SN to cerebral cortex in the internal capsule, from other potential paths that do not travel in the internal capsule and/or passing through the basal ganglia (and as such would not be direct). We excluded thalamus, caudate, putamen, globus pallidum (GP), STN, and corpus callosum. Since the putamen and pallidus were used as ROAs, it was fundamental that they did not include part of the internal capsule; indeed, the mask of these two regions were manually drawn by keeping only voxels with FA values lower than 0.2. This step was performed to exclude from the analysis fibers passing through the basal ganglia (Grèzes et al., 2014).

For visualization purposes, we reconstructed a color-coded map in which red, blue, and green colors indicate the principal streamline directions (Pajevic and Pierpaoli, 1999). Specifically, red color indicates a latero-lateral pattern, green color an anterior-posterior pattern, and blue color a caudal-cranial pattern. Intensity and pureness of these colors vary according to the behavior of fiber bundles in all intermediate positions.

Analysis of Diffusion Tensor Parameters

We extracted for each pathway mean fractional anisotropy (FA) parameter defined by Basser (1995). Diffusion tensors were estimated with a non-linear procedure, which allowed to minimize unrealistic results (Jones and Basser, 2004), by means of CAMINO software package (<http://cmic.cs.ucl.ac.uk/camino/>). By using in-house scripts built with MATLAB software package (<http://www.mathworks.com>), we extracted FA for each pathway.

Connectivity Analysis

Once whole brain probabilistic tractography process terminated, for each subject we isolated streamlines linking SN with cortical areas previously parcellated on structural scans. Then, we calculated number of streamlines connecting each couple of ROIs. With some limitations (Smith et al., 2013), such numbers are used as markers of connectivity density, both in healthy and pathological conditions (Behrens and Sporns, 2012; Bijttebier et al., 2015; Li et al., 2016).

This approach is defective since streamlines are generated without considering the amount of white matter they represent and information such as the size of ROIs and the distance between ROIs.

Then we took into account for volume and distance biases, since it is documented that streamlines are more likely to connect with larger ROIs or closer ROIs. In this sense, we performed weighted connectivity defined as the density of the streamlines linking a couple of ROIs, which definitely is the number of tracts scaled by the sum of inverse of the fiber length and the mean volume of two ROIs (Cheng et al., 2012).

Statistical Analysis

Statistical analyses were conducted using STATA version 13.0 (StataCorp, Colleague Station, Texas, USA) and SigmaPlot v11.0 (Systat Software Inc., Germany). Data were checked for errors and normality assessed for all continuous variables. All data sets were found to be normally distributed.

Paired *t*-tests were used to assess differences between left and right cortical connectivity of SN and between left and right FA values, and unpaired *t*-tests to assess the differences in cortical connectivity between male and female. Reported *P*-values have not been corrected for multiple comparisons, but a *P*-value was considered to be significant only after Bonferroni's correction for multiple comparisons for each of the 33 areas considered (i.e., $P < 0.0015$).

Pearson's correlation was used to test correlations between connectivity and FA for significance. All tests were two-sided.

RESULTS

In our cohort ($n = 15$), 7 of the subjects were women, the average age was 35.46 ± 11 years.

Thirty-three consistent patterns of CSD tractography-based structural cortical connectivity from the left and right SN were identified (Figure 2). The vast majority of the cortico-nigral connectivity (~83%) was directed toward 8 cortical areas, namely, superior frontal (~25%; Figure 3A), precentral (15.4%; Figure 3B), pars triangularis (10.8%; Figure 3C), rostral middle frontal (7.9%; Figure 3D), pars orbitalis (6.7%; Figure 3C), pars opercularis (7.2%; Figure 3C), paracentral (6.8%; Figure 3E), postcentral (3.6%; Figure 3F; average of the right and left side).

Significant differences were found between left and right cortical connectivity of SN of the caudal middle frontal ($p < 0.0001$), pars opercularis ($p < 0.0001$), posterior cingulate ($p < 0.0001$), rostral middle frontal ($p < 0.0001$), pars orbitalis ($p = 0.0003$), superior frontal ($p = 0.0002$). The pars opercularis, pars orbitalis and rostral middle frontal were predominant right sided, while the others left sided (Figure 4). There was no correlation between connectivity and FA. Connectivity was not associated with gender and did not correlate with age.

In particular, the cortico-nigral fibers ran within the internal capsule to the cerebral peduncle, and finally reached the SN in ventral midbrain (Figure 5; Supplementary Figure 1).

Left and right mean FA values are shown in Table 1, whilst Table 2 summarizes our data in comparison to data obtained in animals.

DISCUSSION

SN can be anatomically and functionally divided in two sections, the antero-lateral SNr and the postero-medial SNC with significant differences in connectivity profile, receptor-architectonics, and functions (Voorn et al., 2004; Guatteo et al.,

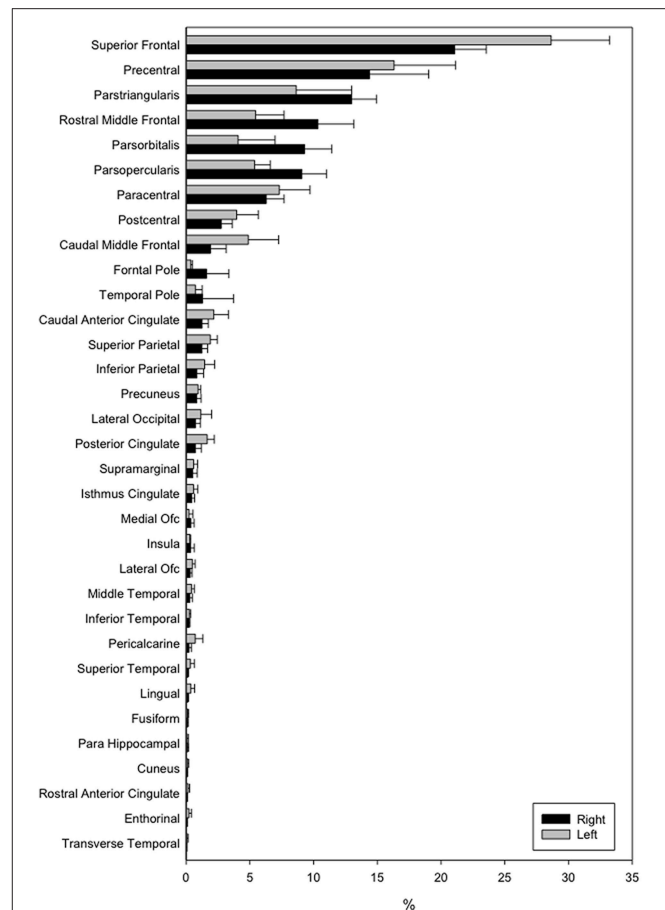


FIGURE 2 | Connectivity results visualized by means of a bar-graph.

2009; Menke et al., 2010; Zhou and Lee, 2011; Chowdhury et al., 2013).

In the present study, we confirmed the existence of an extensive neural pathway running between cerebral cortex and SN, as described by existing literature.

In particular, we noticed the highest connectivity profile for SN with SFG, which is known to be an important prefrontal area; in addition, lower values of connectivity were found between SN and other prefrontal areas areas such as pars opercularis, pars orbitalis, pars triangularis, and rostral MFG. These findings are in line with data regarding PFC-SN connectivity described in rodents (Bunney and Aghajanian, 1976; Kornhuber, 1984; Sesack et al., 1989) and primates (Leichnetz and Astruc, 1976; Künzle, 1978; Frankle et al., 2006), and with the few existing results obtained in humans by means of DTI-based techniques (Menke et al., 2010; Kwon and Jang, 2014). Interestingly, connections between PFC and SN in humans appears to be more prominent and represented than the sparse dPFC/SN projections described by Frankle and colleagues in macaca monkeys. On the other hand, we were not able to find representative connections between OFC and SN, in contrast to findings revealed in primates (Frankle et al., 2006).

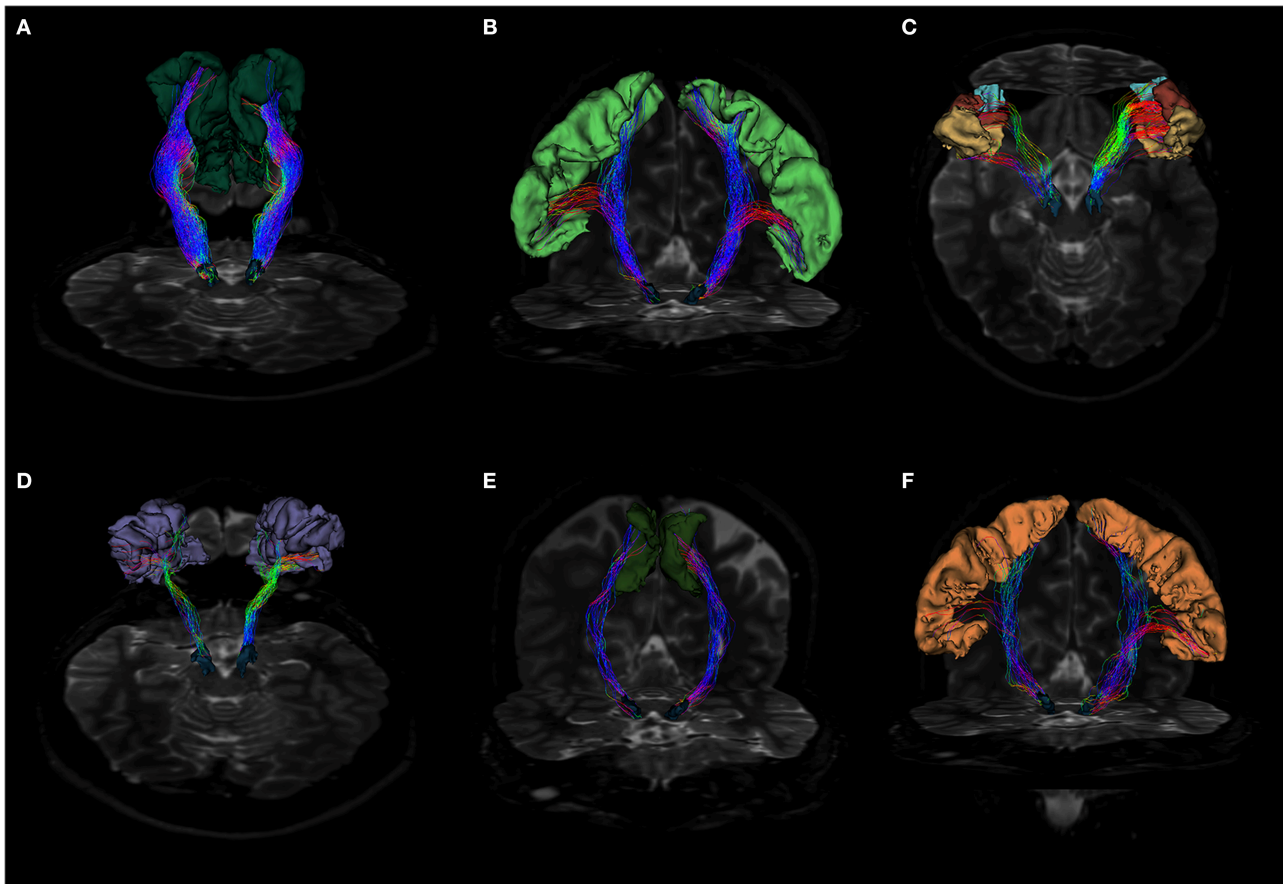


FIGURE 3 | (A) Fiber tracts between SN and superior frontal gyrus visualized in a posterior coronal view. SN model is represented in blue, while SFG is colored in dark green. Notice the rich density and organization of these connections. (B) Anterior coronal view of fibers between SN and precentral gyrus. SN model is shown in blue, precentral gyrus in pale green. Fiber tracts run through the internal capsule and reach preferentially the posterior and lateral parts of SN. (C) Fiber tracts between SN and pars opercularis, pars triangularis and pars orbitalis. SN model is shown in blue, pars opercularis in yellow, pars triangularis in brown and pars orbitalis in light blue. Fibers run through the internal capsule and reach the anterior part of SN. (D) Posterior view of fiber tracts between SN and rostral middle frontal gyrus. SN is depicted in blue, while rMFG in pale purple. Streamlines mainly approach the anterior part of SN. (E) Fiber tracts between SN and paracentral lobule in anterior coronal view. SN is shown in blue, SMA in green. Fiber tracts mainly interest the posterior part of SN. (F) Fiber tracts between SN and postcentral gyrus visualized in anterior coronal view. SN model is depicted in blue, postcentral gyrus in orange. Streamlines spread mainly from the medial regions of postcentral gyrus, but also from the most infero-lateral ones.

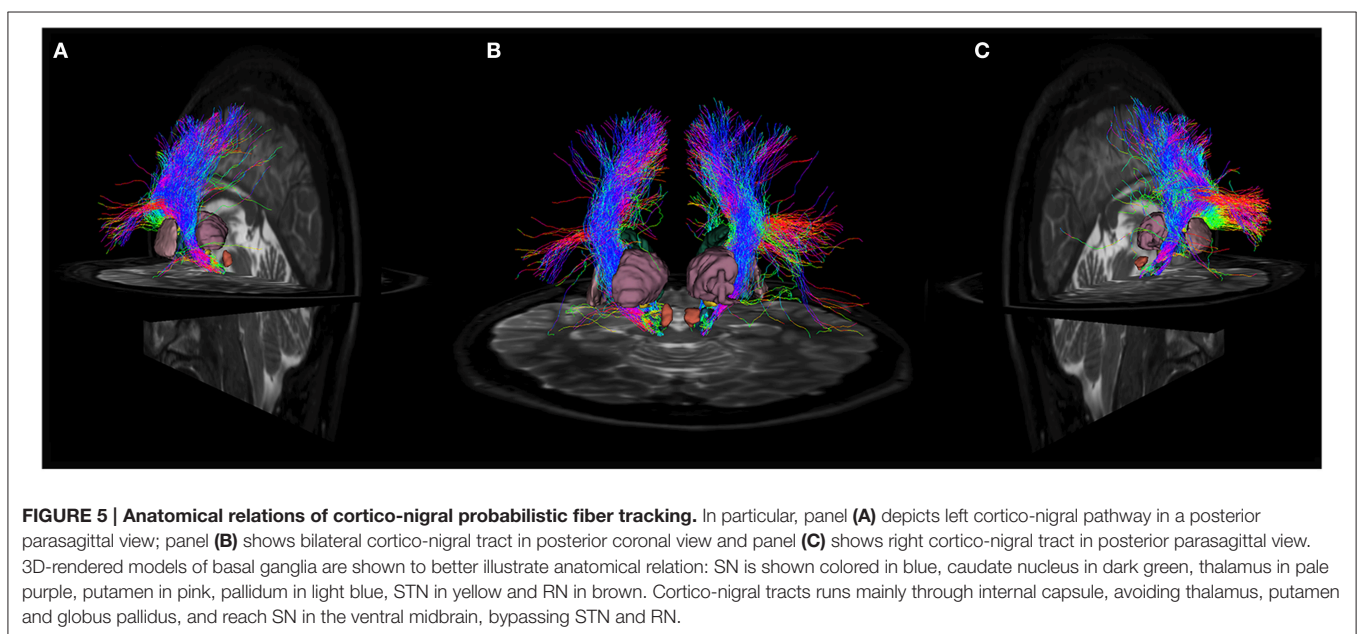
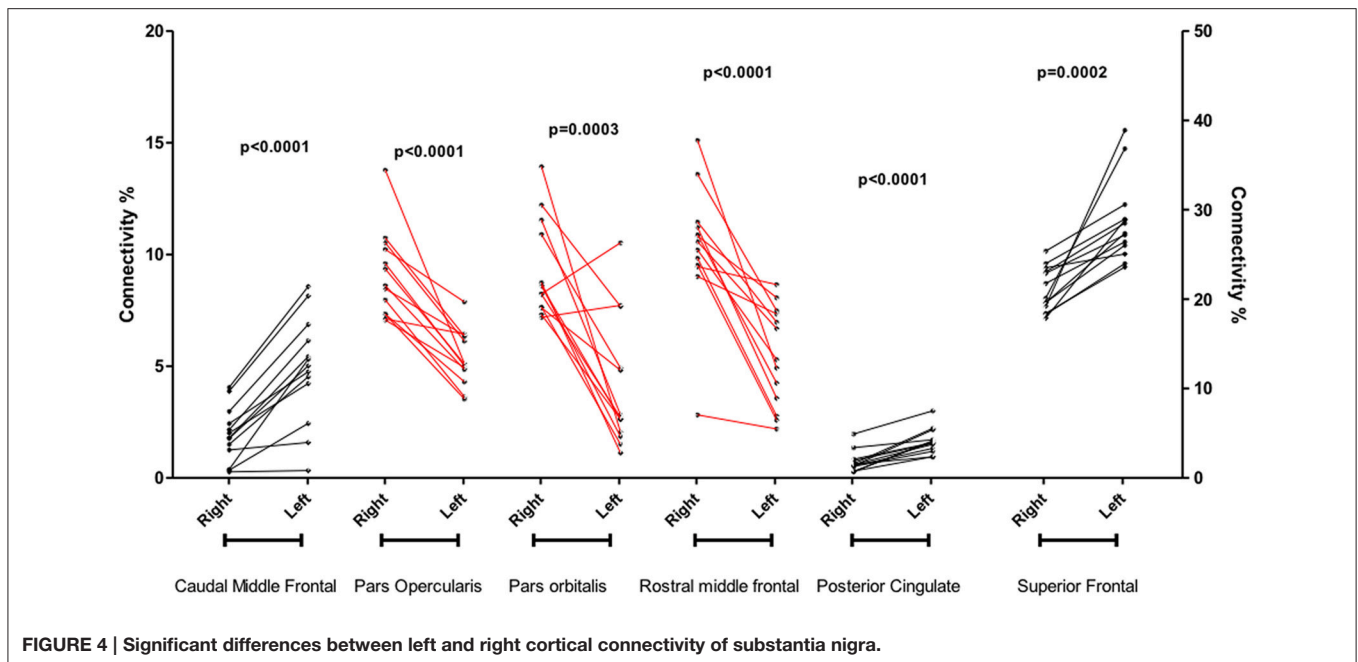
We also found well-represented connections between SN and cortical areas related with motor functions, such as paracentral lobule and precentral gyrus: this finding is in line with the existing literature that revealed sparse connections between motor cortex, premotor cortex and SN in primates (Künzle, 1978; von Monakow et al., 1979).

In a recent study aimed to examine functional networks related to the extrapyramidal system by using fMRI, it was shown that SN is connected with supplementary motor area (SMA), suggesting the former as an activity driver of the SMA and the latter as a crucial node within the cortico-basal network (Zhang et al., 2015).

Finally, we found significant connections between SN with parietal sensory and sensory-motor cortices. These findings are in keeping with animal data in rodents, obtained with anterograde

tracers, that have shown extensive connections running from primary somatosensory area to SNr (Zakiewicz et al., 2014).

This is not the first attempt in demonstrating connections between cerebral cortex and SN in humans. Hence, the existence of direct cortico-nigral fibers has been postulated and demonstrated, back to the first half of XX century, by the French anatomist Leo Testut who, in its classical textbook of anatomy, comments: “Fibers of cerebral cortex, coming from the rolandic region, pass through the internal capsule, with the peduncular pathway, reach the peduncle’s foot and enter the anterior part of SN” (Testut and Latarjet, 1971). A recent study found that SN could be likely connected with prefrontal cortex and sensory-motor cortex, but the authors concluded that these connections were not linking cortex and SN directly, but passing through thalamus (Menke et al., 2010).



By using a probabilistic tractography method based on a multi-fiber model, Kwon and Jang (2014) demonstrated that SN showed high connectivity values to primary motor cortex, primary somatosensory cortex, and premotor cortex and prefrontal cortex. As claimed by the authors, their study suffered from intrinsic technical DTI limitations (Parker and Alexander, 2005; Fillard et al., 2011; Jeurissen et al., 2013) and MRI data were acquired with low Tesla (1.5), channels (6), and diffusion directions (32).

In the present paper, we used a HARDI-CSD-based technique, which is able to provide more robust data, estimating

one or more fiber orientations in presence of intravoxel orientational heterogeneity (Tournier et al., 2007, 2008). Moreover, we acquired MRI data with a 3T scanner, 32 channels, b -value = 1500 s/mm², and 64 gradient diffusion directions, improving quality of data and reliability of results. Finally, in our work we used exclusion masks for caudate, putamen, thalamus, globus pallidus and STN, and therefore we can assume that this cortico-nigral connectivity is likely to be direct.

Several evidences reinforce the presence of direct cortico-nigral projections in humans. It has been reported that the

TABLE 1 | Significant differences between left and right mean FA values.

FA	Right	Left	P-value
Caudal anterior cingulate	0.49 ± 0.041	0.49 ± 0.041	ns
Caudal middle frontal	0.43 ± 0.016	0.43 ± 0.031	ns
Cuneus	0.49 ± 0.031	0.48 ± 0.033	ns
Enthorinal	0.47 ± 0.029	0.47 ± 0.044	ns
Fusiform	0.48 ± 0.023	0.48 ± 0.019	ns
Inferior parietal	0.43 ± 0.024	0.44 ± 0.024	ns
Inferior temporal	0.47 ± 0.022	0.47 ± 0.008	ns
Isthmus cingulate	0.49 ± 0.026	0.49 ± 0.035	ns
Lateral occipital	0.46 ± 0.027	0.45 ± 0.029	ns
Lateral OFC	0.46 ± 0.035	0.47 ± 0.022	ns
Lingual	0.48 ± 0.036	0.47 ± 0.029	ns
Medial OFC	0.48 ± 0.035	0.48 ± 0.023	ns
Middle temporal	0.46 ± 0.017	0.46 ± 0.014	ns
Para hippocampal	0.49 ± 0.028	0.49 ± 0.024	ns
Paracentral	0.42 ± 0.016	0.45 ± 0.023	0.0002
Parsopercularis	0.43 ± 0.018	0.44 ± 0.026	ns
Parsorbitalis	0.42 ± 0.076	0.46 ± 0.023	ns
Parstriangularis	0.42 ± 0.022	0.44 ± 0.034	0.0005
Pericalcarine	0.48 ± 0.043	0.47 ± 0.031	ns
Postcentral	0.42 ± 0.016	0.42 ± 0.021	ns
Posterior cingulate	0.49 ± 0.042	0.49 ± 0.042	ns
Precentral	0.39 ± 0.015	0.4 ± 0.021	ns
Precuneus	0.44 ± 0.023	0.45 ± 0.024	ns
Rostral anterior cingulate	0.5 ± 0.035	0.51 ± 0.032	ns
Rostral middle frontal	0.4 ± 0.016	0.41 ± 0.031	ns
Superior frontal	0.39 ± 0.016	0.4 ± 0.034	ns
Superior parietal	0.42 ± 0.025	0.42 ± 0.02	ns
Superior temporal	0.46 ± 0.018	0.46 ± 0.016	ns
Supramarginal	0.44 ± 0.024	0.45 ± 0.026	ns
Forntal pole	0.48 ± 0.037	0.47 ± 0.023	ns
Temporal pole	0.46 ± 0.032	0.46 ± 0.029	ns
Transverse temporal	0.5 ± 0.034	0.5 ± 0.032	ns
Insula	0.47 ± 0.021	0.47 ± 0.017	ns

ns, non-significant.

unilateral ablation of PFC causes a significant reduction of glutamate levels in the ipsilateral SN (Kornhuber, 1984). In addition, there is an old paper suggesting that the pacemaker-like activity of SN neurons can be modulated by afferent cortical projections (Gariano and Groves, 1988).

Finally, there are also indirect evidences suggesting the presence of cortico-nigral connections in humans. Indeed, Strafella and co-workers demonstrated that repetitive transcranial magnetic stimulation over primary motor area and PFC induces dopamine release in caudate nucleus (Strafella et al., 2001).

Physiopathological Implications

The well-known model of basal ganglia physiology put forward by DeLong in the late eighties has plagued the field with a paramount impact on the comprehension of movement disorders (MD), which has boosted neurosurgery for these conditions

TABLE 2 | Comparison between our findings in human brain and other results animal brain.

Areas involved in rats	Areas involved in primates	Areas involved in humans
Medial prefrontal cortex (Sesack et al., 1989)	Orbital prefrontal cortex, dorso lateral prefrontal cortex, cingulate cortex (Frankle et al., 2006)	Superior frontal gyrus
Prefrontal cortex, with sparse fibers to insular, parietal, and temporal cortex (Bunney and Aghajanian, 1976)	Area 6 and area 9 (Künzle, 1978; von Monakow et al., 1979)	Precentral gyrus
Motor and premotor areas (Kornhuber, 1984)		Pars triangularis
Orbital area, prelimbic rostral area, anterior cingulate area (Beckstead, 1979; Naito and Kita, 1994)		Rostral middle frontal gyrus
Rostral agranular insular cortex (Jasmin et al., 2004)		Pars orbitalis
Primary somatosensory area (Zakiewicz et al., 2014)		Pars opercularis
Olfactory cortex (Höglinger et al., 2015)		Paracentral gyrus
		Postcentral gyrus

For animal findings, we maintained the anatomical nomenclature found in original research articles. References are discussed in text body.

(DeLong, 1990). The essence of the model postulates that cortical information flows through the basal ganglia via two major systems: the direct and indirect pathways, originating from segregated populations of striatal medium spiny neurons (MNs) and exerting opposite effects on basal ganglia outflow.

In particular it has been shown that that selective stimulation of the indirect pathway (D1 receptors) provoked movement arrest while activation of direct pathway (D2 receptors) led to movement activation (Bateup et al., 2010).

In addition to the striatum another important node of the network is the STN, which has extensive cortical connections through a fast conductive cortico-subthalamic pathway called hyper-direct pathway (Nambu et al., 2002; Nambu, 2005).

In a recent paper, we have challenged the traditional model of basal ganglia functioning by showing the existence of cortico-pallidal projections in humans (Milardi et al., 2015). By using a CSD-based tractographic approach, we demonstrated the presence of direct pathways connecting Brodmann's areas 4, 5, 6, 11, 12, 46, and 48 with both segments of GP. The cortical output to both segments of GP may provide an efficient system to control upstream direct and indirect pathways. These findings are substantially in line with the emerging view on basal ganglia organization, also supported by several tractographic studies (Draganski et al., 2008; Lambert et al., 2012).

This pathway may provide direct cortical access to GP, bypassing the striatum, and may represent an additional route for cortical regulation of the basal ganglia circuitry (Smith and Wichmann, 2015).

Interestingly, a magnetoencephalography study has recently identified in dystonia patients a robust band of beta coherence between motor and premotor cortical areas with GPi, confirming the functional role of cortico-pallidal beta signaling in regulating

the cortex-basal ganglia-cortex feedback loops implicated in motor control (Neumann et al., 2015). We have recently also proposed a new framework where the existence of this abnormal cortico-pallidal connectivity should be explored at a functional and structural level to shed new light on the pathophysiology of movement disorders (Cacciola et al., 2016). In this scenario, we speculated that, as the hyperdirect pathway is a faster connection of cortex with STN, with respect to the direct and indirect pathways, similarly the cortico-pallidal fibers could represent a fast connection between cortex and GP (Milardi et al., 2015; Cacciola et al., 2016).

In the present paper, we provide new evidences supporting the existing model of basal ganglia network physiology by means of tractographic demonstration of a complementary direct cortico-SN pathway that could work paralleling the cortico-pallidal system.

This direct cortico-nigral system is likely to be a very important hierarchically node within the basal ganglia network, as it may exert a powerful upstream control on direct and indirect pathways through a modulation of the nigro-striatal system in addition to the cortico-GPi direct pathway. In addition, we have recently shown a direct connectivity between cerebellum and SN, which may represent a fast route for cerebellar activity to regulate and to be regulated by basal ganglia activity (Milardi et al., 2016a). In this perspective, cortico-nigral-cerebellar connections may directly interact each other resulting in a fine regulation of SNr firing.

However, based on MRI data used in the present study, we cannot discriminate between the two different portions of SN.

SNr is, along with internal globus pallidus (GPi), the output nucleus in basal ganglia circuitry, since it fires directly on VA and VL thalamic nuclei with inhibitory GABA-ergic neurons. The regular high-frequency spontaneous firing of SNr neurons is mainly modulated by inhibitory neurons from striatum and external globus pallidus (GPe) and excitatory neurons from STN (Zhou and Lee, 2011).

The results of the present study are very relevant in light of recent findings that have demonstrated an important role of SNr in the pathophysiology of hyperkinetic MD providing an explanation of the paradox of pallidotomy in PD. It is well-known that, according to the traditional model of DeLong, a lesion of the GP should reduce GPi efferent activity worsening the dyskinesias (DeLong, 1990). However, clinical data in several hundreds of treated patients suggest the opposite (Bejjani et al., 1997; Guridi and Lozano, 1997; Lozano and Lang, 2001; Wu et al., 2001; Volkmann et al., 2002; Munhoz et al., 2014).

A partial solution of this paradox has been provided by Dybdal and colleagues who have demonstrated that experimental inhibition of a very restricted area of SNr can induce a choreiform dyskinesia which is distinct from that responsible for inducing torticollis (Dybdal et al., 2013).

The contralateral directed choreiform dyskinesias and torticollis observed after focal inhibition within specific regions of the SNr can explain some of the symptoms observed in several MD such as, Huntington's disease, levodopa-induced dyskinesias, cranio-cervical and generalized dystonias, and tardive dyskinesias and dystonias.

The crucial role of SNr in MD can also explain why the excessive activation of glutamatergic subthalamo-SNr and GABAergic pallido-SNr fibers, driven by STN DBS may produce dyskinesias (Bosch et al., 2011).

Strategies aimed at disinhibition of the SNr warrant further exploration as potential therapeutic interventions for human torticollis and dyskinetic syndromes. In this perspective, cortical modulation with non-invasive neuromodulation technique could offer an alternative opportunity to modulate SN firing.

LIMITATIONS

The present study regarding cerebral-SN connectivity suffers from some limitations. It is worthy to note that tractography does not provide a direct visualization of axons, allowing only a probabilistic representation of the most likely trajectories based on local diffusion.

A drawback of this technique is also the inability to establish the directionality of signal transmission (Chung et al., 2011; Parker et al., 2013) that need to be determined with functional connectivity approaches. The latter could use technique such as dynamic causal modeling to infer whether firing of one brain region leads to activity changes in other regions, thus determining directionality of these connections. A combined approach between dynamic causal modeling-based functional studies together with the tracking method employed in the present study, should be fostered to resolve issue directionality of this cortico-basal ganglia pathway. Moreover, tractography cannot provide fully conclusive evidence of direct anatomical connections since it is unable to disentangle monosynaptic from polysynaptic connections and to detect gap junctions. Further studies need to be carried out in the human brain using postmortem microsurgery dissection and/or tracer injection or *in vivo* fMRI in order to confirm the existence of this cortico-nigral pathway.

A further limitation of the present study is that we could not discriminate between cortical direct connectivity of SNc and SNr, since images resolution didn't allow for it. However, this could be the aim of further investigations, by using higher resolution acquisition and 7T scanners.

Although our results are anatomically plausible compared with previous anatomical descriptions of these connections in animals, tractography results have to be interpreted with caution. Hence, it is well-known that tractography may suffer from reconstruction biases, such as possible false positive streamlines. In this regard, to make our tractographic findings more reliable we decided to use probabilistic CSD tractography with more conservative reconstruction criteria respecting usual standard (Descoteaux et al., 2009; Milardi et al., 2015), at the cost of an underestimation issue.

Finally, our results are based on a relatively small sample of adult subjects, and this might explain why we have not found any correlations between sex and age.

However, despite its limitations, it is worthy to remember that tractography is the only available technique to investigate structural neural connectivity *in vivo* and non-invasively.

CONCLUSIONS

Using diffusion-tensor magnetic resonance imaging and CSD tractography, we demonstrated the presence of direct anatomical cortico-nigral connections, already extensively described in cats, rodents and primates but only suggested in humans.

This direct connection might be another piece of the puzzle toward a more extensive comprehension of cortical regulation on both motor basal ganglia and dopaminergic reward circuits and might pave the way for further biochemical and physiological investigations.

AUTHOR CONTRIBUTIONS

AC: Study concepts/study design, data acquisition, data analysis, data interpretation, literature research. DM: Study concepts/study design, manuscript revision. GA: Guarantor of integrity of entire study, approval of final version of submitted manuscript, data interpretation. GB: Data analysis, data interpretation, literature research, statistical analysis. MI: Data analysis, literature research, statistical analysis. PC: Data analysis, data interpretation. GC: Literature

REFERENCES

- Afifi, A. K., Bahuth, N. B., Kaelber, W. W., Mikhael, E., and Nassar, S. (1974). The cortico-nigral fibre tract. An experimental Fink-Heimer study in cats. *J. Anat.* 118, 469–476.
- Alexander, D. C., and Barker, G. J. (2005). Optimal imaging parameters for fiber-orientation estimation in diffusion MRI. *Neuroimage* 27, 357–367. doi: 10.1016/j.neuroimage.2005.04.008
- Basser, P. J. (1995). Inferring microstructural features and the physiological state of tissues from diffusion-weighted images. *NMR Biomed.* 8, 333–344. doi: 10.1002/nbm.1940080707
- Basser, P. J., Mattiello, J., and LeBihan, D. (1994). MR diffusion tensor spectroscopy and imaging. *Biophys. J.* 66, 259–267. doi: 10.1016/S0006-3495(94)80775-1
- Bateup, H. S., Santini, E., Shen, W., Birnbaum, S., Valjent, E., Surmeier, D. J., et al. (2010). Distinct subclasses of medium spiny neurons differentially regulate striatal motor behaviors. *Proc. Natl. Acad. Sci. U.S.A.* 107, 14845–14850. doi: 10.1073/pnas.1009874107
- Beckstead, R. M. (1979). An autoradiographic examination of corticocortical and subcortical projections of the mediodorsal-projection (prefrontal) cortex in the rat. *J. Comp. Neurol.* 184, 43–62. doi: 10.1002/cne.901840104
- Behrens, T. E., Berg, H. J., Jbabdi, S., Rushworth, M. F., and Woolrich, M. W. (2007). Probabilistic diffusion tractography with multiple fibre orientations: what can we gain? *Neuroimage* 34, 144–155. doi: 10.1016/j.neuroimage.2006.09.018
- Behrens, T. E., and Sporns, O. (2012). Human connectomics. *Curr. Opin. Neurobiol.* 22, 144–153. doi: 10.1016/j.conb.2011.08.005
- Bejjani, B., Damier, P., Arnulf, I., Bonnet, A. M., Vidailhet, M., Dormont, D., et al. (1997). Pallidal stimulation for Parkinson's disease. Two targets? *Neurology* 49, 1564–1569. doi: 10.1212/WNL.49.6.1564
- Besson, P., Dinklacker, V., Valabregue, R., Thivard, L., Leclerc, X., Baulac, M., et al. (2014). Structural connectivity differences in left and right temporal lobe epilepsy. *Neuroimage* 100, 135–144. doi: 10.1016/j.neuroimage.2014.04.071
- Bijttebier, S., Caeyenberghs, K., van den Amele, H., Achten, E., Rujescu, D., Titeca, K., et al. (2015). The vulnerability to suicidal behavior is associated with reduced connectivity strength. *Front. Hum. Neurosci.* 9:632. doi: 10.3389/fnhum.2015.00632
- Bosch, C., Degos, B., Deniau, J. M., and Venance, L. (2011). Subthalamic nucleus high-frequency stimulation generates a concomitant synaptic excitation-inhibition in substantia nigra pars reticulata. *J. Physiol.* 589(Pt 17), 4189–4207. doi: 10.1113/jphysiol.2011.211367
- Bunney, B. S., and Aghajanian, G. K. (1976). The precise localization of nigral afferents in the rat as determined by a retrograde tracing technique. *Brain Res.* 117, 423–435. doi: 10.1016/0006-8993(76)90751-4
- Cacciola, A., Milardi, D., and Quartarone, A. (2016). Role of cortico-pallidal connectivity in the pathophysiology of dystonia. *Brain*. doi: 10.1093/brain/aww102. [Epub ahead of print].
- Carman, J. B. (1968). Anatomic basis of surgical treatment of Parkinson's disease. *N. Engl. J. M.* 17, 919–930. doi: 10.1056/NEJM196810242791706
- Carter, C. J. (1982). Topographical distribution of possible glutamatergic pathways from the frontal cortex to the striatum and substantia nigra in rats. *Neuropharmacology* 21, 379–383. doi: 10.1016/0028-3908(82)90019-3
- Cheng, H., Wang, Y., Sheng, J., Kronenberger, W. G., Mathews, V. P., Hummer, T. A., et al. (2012). Characteristics and variability of structural networks derived from diffusion tensor imaging. *Neuroimage* 61, 1153–1164. doi: 10.1016/j.neuroimage.2012.03.036
- Chowdhury, R., Lambert, C., Dolan, R. J., and Düzel, E. (2013). Parcellation of the human substantia nigra based on anatomical connectivity to the striatum. *Neuroimage* 81, 191–198. doi: 10.1016/j.neuroimage.2013.05.043
- Chung, H. W., Chou, M. C., and Chen, C. Y. (2011). Principles and limitations of computational algorithms in clinical diffusion tensor MR tractography. *Am. J. Neuroradiol.* 32, 3–13. doi: 10.3174/ajnr.A2041
- DeLong, M. R. (1990). Primate models of movement disorders of basal ganglia origin. *Trends Neurosci.* 13, 281–285. doi: 10.1016/0166-2236(90)90110-V
- Descoteaux, M., Deriche, R., Knösche, T. R., and Anwander, A. (2009). Deterministic and probabilistic tractography based on complex fibre orientation distributions. *IEEE Trans. Med. Imaging.* 28, 269–286. doi: 10.1109/TMI.2008.2004424
- Desikan, R. S., Ségonne, F., Fischl, B., Quinn, B. T., Dickerson, B. C., Blacker, D., et al. (2006). An automated labeling system for subdividing the human cerebral cortex on MRI scans into gyral based regions of interest. *Neuroimage* 31, 968–980. doi: 10.1016/j.neuroimage.2006.01.021
- Draganski, B., Kherif, F., Klöppel, S., Cook, P. A., Alexander, D. C., Parker, G. J., et al. (2008). Evidence for segregated and integrative connectivity

research. DB: Literature research. GR: Data acquisition. SM: Statistical analysis, data analysis. PB: Manuscript revision. AQ: Study concepts/study design, guarantor of integrity of entire study, manuscript revision for important intellectual content.

ACKNOWLEDGMENTS

We would like to thank Prof. Placido Bramanti, Science Manager of I.R.C.C.S. “Centro Neurolesi,” Messina, Italy, for the helpful collaboration, and Alessandro Calamuneri, MSc, Ph.D for the helpful technical suggestions for elaborating MRI data.

SUPPLEMENTARY MATERIAL

The Supplementary Material for this article can be found online at: <http://journal.frontiersin.org/article/10.3389/fnhum.2016.00374>

Supplementary Figure 1 | Course of cortico-nigral connections.

Representation of the course of the connections between cerebral cortex and SN. On the right fibers are red colored, on the left blue colored. The first two images depict tracts leaving the cerebral cortex, then fibers pass through corona radiata and internal capsule to finally reach SN.

- patterns in the human basal ganglia. *J. Neurosci.* 28, 7143–7152. doi: 10.1523/JNEUROSCI.1486-08.2008
- Düzel, E., Bunzeck, N., Guitart-Masip, M., Wittmann, B., Schott, B. H., and Tobler, P. N. (2009). Functional imaging of the human dopaminergic midbrain. *Trends Neurosci.* 32, 321–328. doi: 10.1016/j.tins.2009.02.005
- Dybdal, D., Forcelli, P. A., Dubach, M., Oppedisano, M., Holmes, A., Malkova, L., et al. (2013). Topography of dyskinesias and torticollis evoked by inhibition of substantia nigra pars reticulata. *Mov. Disord.* 28, 460–468. doi: 10.1002/mds.25215
- Embleton, K. V., Haroon, H. A., Morris, D. M., Ralph, M. A., and Parker, G. J. (2010). Distortion correction for diffusion-weighted MRI tractography and fMRI in the temporal lobes. *Hum. Brain Mapp.* 31, 1570–1587. doi: 10.1002/hbm.20959
- Farquharson, S., Tournier, J. D., Calamante, F., Fabbinyi, G., Schneider-Kolsky, M., Jackson, G. D., et al. (2013). White matter fiber tractography: why we need to move beyond DTI. *J. Neurosurg.* 118, 1367–1377. doi: 10.3171/2013.2.JNS.121294
- Fillard, P., Descoteaux, M., Goh, A., Gouttard, S., Jeurissen, B., Malcolm, J., et al. (2011). Quantitative evaluation of 10 tractography algorithms on a realistic diffusion MR phantom. *Neuroimage* 56, 220–234. doi: 10.1016/j.neuroimage.2011.01.032
- Fischl, B., and Dale, A. M. (2000). Measuring the thickness of the human cerebral cortex from magnetic resonance images. *Proc. Natl. Acad. Sci. U.S.A.* 97, 11050–11055. doi: 10.1073/pnas.200033797
- Fischl, B., Salat, D. H., van der Kouwe, A. J., Makris, N., Ségonne, F., Quinn, B. T., et al. (2004). Sequence-independent segmentation of magnetic resonance images. *Neuroimage* 23(Suppl. 1), S69–S84. doi: 10.1016/j.neuroimage.2004.07.016
- Foix, C., and Niclescu, I. T. (1925). *Anatomie Cérébrale; Les Noyaux Gris Centraux et la Région Mésencéphalo-Sous-Optique, Suivi d'un Appendice sur l'anatomie Pathologique de la Maladie de Parkinson*. Paris: Masson et cie.
- Frankle, W. G., Laruelle, M., and Haber, S. N. (2006). Prefrontal cortical projections to the midbrain in primates: evidence for a sparse connection. *Neuropsychopharmacology* 31, 1627–1636. doi: 10.1038/sj.npp.1300990
- Gariano, R. F., and Groves, P. M. (1988). Burst firing induced in midbrain dopamine neurons by stimulation of the medial prefrontal and anterior cingulate cortices. *Brain Res.* 462, 194–198. doi: 10.1016/0006-8993(88)90606-3
- Grézes, J., Valabrègue, R., Gholipour, B., and Chevallier, C. (2014). A direct amygdala-motor pathway for emotional displays to influence action: a diffusion tensor imaging study. *Hum. Brain Mapp.* 35, 5974–5983. doi: 10.1002/hbm.22598
- Guatteo, E., Cucchiaroni, M. L., and Mercuri, N. B. (2009). Substantia nigra control of basal ganglia nuclei. *J. Neural Transm. Suppl.* 73, 91–101. doi: 10.1007/978-3-211-92660-4_7
- Guridi, J., and Lozano, A. M. (1997). A brief history of pallidotomy. *Neurosurgery* 41, 1169–1180. doi: 10.1097/00006123-199711000-00029
- Henderson, J. M. (2012). “Connectomic surgery”: diffusion tensor imaging (DTI) tractography as a targeting modality for surgical modulation of neural networks. *Front. Integr. Neurosci.* 6:15. doi: 10.3389/fnint.2012.00015
- Höglinger, G. U., Alvarez-Fischer, D., Arias-Carrión, O., Djufri, M., Windolph, A., Keber, U., et al. (2015). A new dopaminergic nigro-olfactory projection. *Acta Neuropathol.* 130, 333–348. doi: 10.1007/s00401-015-1451-y
- Jang, S. H., Son, S. M., Lee, D. Y., and Hong, J. H. (2013). Relationship between somatosensory function and the spinothalamic pathway in chronic stroke patients. *Somatosens. Mot. Res.* 30, 197–200. doi: 10.3109/08990220.2013.790808
- Jasmin, L., Granato, A., and Ohara, P. T. (2004). Rostral agranular insular cortex and pain areas of the central nervous system: a tract-tracing study in the rat. *J. Comp. Neurol.* 468, 425–440. doi: 10.1002/cne.10978
- Jbabdi, S., and Johansen-Berg, H. (2011). Tractography: where do we go from here? *Brain Connect.* 1, 169–183. doi: 10.1089/brain.2011.0033
- Jbabdi, S., Sotiropoulos, S. N., Haber, S. N., Van Essen, D. C., and Behrens, T. E. (2015). Measuring macroscopic brain connections *in vivo*. *Nat. Neurosci.* 18, 1546–1555. doi: 10.1038/nn.4134
- Jeurissen, B., Leemans, A., Tournier, J. D., Jones, D. K., and Sijbers, J. (2013). Investigating the prevalence of complex fiber configurations in white matter tissue with diffusion magnetic resonance imaging. *Hum. Brain Mapp.* 34, 2747–2766. doi: 10.1002/hbm.22099
- Jones, D. K., and Basser, P. J. (2004). “Squashing peanuts and smashing pumpkins”: how noise distorts diffusion-weighted MR data. *Magn. Reson. Med.* 52, 979–993. doi: 10.1002/mrm.20283
- Jones, D. K., and Cercignani, M. (2010). Twenty-five pitfalls in the analysis of diffusion MRI data. *NMR Biomed.* 23, 803–820. doi: 10.1002/nbm.1543
- Kita, H. (2001). Neostriatal and globus pallidus stimulation induced inhibitory postsynaptic potentials in entopeduncular neurons in rat brain slice preparations. *Neuroscience* 105, 871–879. doi: 10.1016/S0306-4522(01)00231-7
- Kornhuber, J. (1984). The cortico-nigral projection: reduced glutamate content in the substantia nigra following frontal cortex ablation in the rat. *Brain Res.* 322, 124–126. doi: 10.1016/0006-8993(84)91189-2
- Künzle, H. (1978). An autoradiographic analysis of the efferent connections from premotor and adjacent prefrontal regions (areas 6 and 9) in macaca fascicularis. *Brain Behav. Evol.* 15, 185–234. doi: 10.1159/000123779
- Kwon, H. G., and Jang, S. H. (2014). Differences in neural connectivity between the substantia nigra and ventral tegmental area in the human brain. *Front. Hum. Neurosci.* 8:41. doi: 10.3389/fnhum.2014.00041
- Lambert, C., Zrinzo, L., Nagy, Z., Lutti, A., Hariz, M., Foltynie, T., et al. (2012). Confirmation of functional zones within the human subthalamic nucleus: patterns of connectivity and sub-parcellation using diffusion weighted imaging. *Neuroimage* 60, 83–94. doi: 10.1016/j.neuroimage.2011.11.082
- Le Bihan, D., and Johansen-Berg, H. (2012). Diffusion MRI at 25: exploring brain tissue structure and function. *Neuroimage* 61, 324–341. doi: 10.1016/j.neuroimage.2011.11.006
- Leblois, A., Boraud, T., Meissner, W., Bergman, H., and Hansel, D. (2006). Competition between feedback loops underlies normal and pathological dynamics in the basal ganglia. *J. Neurosci.* 26, 3567–3583. doi: 10.1523/JNEUROSCI.5050-05.2006
- Leichnetz, G. R., and Astruc, J. (1976). The efferent projections of the medial prefrontal cortex in the squirrel monkey (*Saimiri sciureus*). *Brain Res.* 109, 455–472. doi: 10.1016/0006-8993(76)90027-5
- Li, C., Huang, B., Zhang, R., Ma, Q., Yang, W., Wang, L., et al. (2016). Impaired topological architecture of brain structural networks in idiopathic Parkinson's disease: a DTI study. *Brain Imaging Behav.* doi: 10.1007/s11682-015-9501-6. [Epub ahead of print].
- Lozano, A. M., and Lang, A. E. (2001). Pallidotomy for Parkinson's disease. *Adv. Neurol.* 86, 413–420.
- McFarland, N. R., and Haber, S. N. (2000). Convergent inputs from thalamic motor nuclei and frontal cortical areas to the dorsal striatum in the primate. *J. Neurosci.* 20, 3798–3813.
- Menke, R. A., Jbabdi, S., Miller, K. L., Matthews, P. M., and Zarei, M. (2010). Connectivity-based segmentation of the substantia nigra in human and its implications in Parkinson's disease. *Neuroimage* 52, 1175–1180. doi: 10.1016/j.neuroimage.2010.05.086
- Milardi, D., Arrigo, A., Anastasi, G., Cacciola, A., Marino, S., Mormina, E., et al. (2016a). Extensive direct subcortical cerebellum-basal ganglia connections in human brain as revealed by constrained spherical deconvolution tractography. *Front. Neuroanat.* 10:29. doi: 10.3389/fnana.2016.00029
- Milardi, D., Cacciola, A., Cutroneo, G., Marino, S., Irrera, M., Cacciola, G., et al. (2016b). Red nucleus connectivity as revealed by constrained spherical deconvolution tractography. *Neurosci. Lett.* 626, 68–73. doi: 10.1016/j.neulet.2016.05.009
- Milardi, D., Gaeta, M., Marino, S., Arrigo, A., Vaccarino, G., Mormina, E., et al. (2015). Basal ganglia network by constrained spherical deconvolution: a possible cortico-pallidal pathway? *Mov. Disord.* 30, 342–349. doi: 10.1002/mds.25995
- Mori, S., Wakana, S., and Van Zijl, P. C. M. (2004). *MRI Atlas of Human White Matter*. Amsterdam, San Diego, CA: Elsevier.
- Mormina, E., Arrigo, A., Calamuner, A., Granata, F., Quartarone, A., Ghilardi, M. F., et al. (2015). Diffusion tensor imaging parameters' changes of cerebellar hemispheres in Parkinson's disease. *Neuroradiology* 57, 327–334. doi: 10.1007/s00234-014-1473-5
- Munhoz, R. P., Cerasa, A., and Okun, M. S. (2014). Surgical treatment of dyskinesia in Parkinson's disease. *Front. Neurol.* 5:65. doi: 10.3389/fneur.2014.00065
- Naito, A., and Kita, H. (1994). The cortico-nigral projection in the rat: an anterograde tracing study with biotinylated dextran amine. *Brain Res.* 637, 317–322. doi: 10.1016/0006-8993(94)91252-1

- Nambu, A. (2005). A new approach to understand the pathophysiology of Parkinson's disease. *J. Neurol.* 252(Suppl. 4), IV1–IV4. doi: 10.1007/s00415-005-4002-y
- Nambu, A., Takada, M., Inase, M., and Tokuno, H. (1996). Dual somatotopical representations in the primate subthalamic nucleus: evidence for ordered but reversed body-map transformations from the primary motor cortex and the supplementary motor area. *J. Neurosci.* 16, 2671–2683.
- Nambu, A., Tokuno, H., Hamada, I., Kita, H., Imanishi, M., Akazawa, T., et al. (2000). Excitatory cortical inputs to pallidal neurons via the subthalamic nucleus in the monkey. *J. Neurophysiol.* 84, 289–300.
- Nambu, A., Tokuno, H., and Takada, M. (2002). Functional significance of the cortico-subthalamo-pallidal 'hyperdirect' pathway. *Neurosci. Res.* 43, 111–117. doi: 10.1016/S0168-0102(02)00027-5
- Nestler, E. J., Hyman, S. E., and Malenka, R. C. (2009). *Molecular Neuropharmacology: A Foundation for Clinical Neuroscience*. New York, NY: McGraw-Hill Medical.
- Neumann, W. J., Jha, A., Bock, A., Huebl, J., Horn, A., Schneider, G. H., et al. (2015). Cortico-pallidal oscillatory connectivity in patients with dystonia. *Brain* 138, 1894–1906. doi: 10.1093/brain/awv109
- Pajevic, S., and Pierpaoli, C. (1999). Colour schemes to represent the orientation of anisotropic tissues from diffusion tensor data: application to white matter fiber tract mapping in the human brain. *Magn. Reson. Med.* 42, 526–540.
- Parker, G. D., Marshall, D., Rosin, P. L., Drage, N., Richmond, S., and Jones, D. K. (2013). A pitfall in the reconstruction of fibre ODFs using spherical deconvolution of diffusion MRI data. *Neuroimage* 65, 433–448. doi: 10.1016/j.neuroimage.2012.10.022
- Parker, G. J., and Alexander, D. C. (2005). Probabilistic anatomical connectivity derived from the microscopic persistent angular structure of cerebral tissue. *Philos. Trans. R. Soc. Lond. B. Biol. Sci.* 360, 893–902. doi: 10.1098/rstb.2005.1639
- Reuter, M., Rosas, H. D., and Fischl, B. (2010). Highly accurate inverse consistent registration: a robust approach. *Neuroimage* 53, 1181–1196. doi: 10.1016/j.neuroimage.2010.07.020
- Rinvik, E. (1966). The cortico-nigral projection in the cat. *Brain Res.* 126, 241–254.
- Sakai, S. T. (1978). Corticonigral projections from area 6 in the raccoon. *Exp. Brain Res.* 73, 498–504. doi: 10.1007/BF00406607
- Segonne, F., Dale, A. M., Busa, E., Glessner, M., Salat, D., Hahn, H. K., et al. (2004). A hybrid approach to the skull stripping problem in MRI. *Neuroimage* 22, 1060–1075. doi: 10.1016/j.neuroimage.2004.03.032
- Ségonne, F., Pacheco, J., and Fischl, B. (2007). Geometrically accurate topology-correction of cortical surfaces using nonseparating loops. *IEEE Trans. Med. Imaging* 26, 518–529. doi: 10.1109/TMI.2006.887364
- Sesack, S. R., Deutch, A. Y., Roth, R. H., and Bunney, B. S. (1989). Topographical organization of the efferent projections of the medial prefrontal cortex in the rat: an anterograde tract-tracing study with Phaseolus vulgaris leucoagglutinin. *J. Comp. Neurol.* 290, 213–242. doi: 10.1002/cne.902900205
- Smith, R. E., Tournier, J. D., Calamante, F., and Connelly, A. (2013). SIFT: spherical-deconvolution informed filtering of tractograms. *Neuroimage* 67, 298–312. doi: 10.1016/j.neuroimage.2012.11.049
- Smith, Y., and Wichmann, T. (2015). The cortico-pallidal projection: an additional route for cortical regulation of the basal ganglia circuitry. *Mov. Disord. M* 30, 293–295. doi: 10.1002/mds.26095
- Strafella, A. P., Paus, T., Barrett, J., and Dagher, A. (2001). Repetitive transcranial magnetic stimulation of the human prefrontal cortex induces dopamine release in the caudate nucleus. *J. Neurosci.* 21, RC157.
- Testut, L., and Latarjet, A. (1971). *Anatomia Umana*. Vol. 3. Torino: UTET.
- Tournier, J. D., Calamante, F., and Connelly, A. (2007). Robust determination of the fibre orientation distribution in diffusion MRI: non-negativity constrained super-resolved spherical deconvolution. *Neuroimage* 35, 1459–1472. doi: 10.1016/j.neuroimage.2007.02.016
- Tournier, J. D., Calamante, F., and Connelly, A. (2011). Effect of step size on probabilistic streamlines: implications for the interpretation of connectivity analysis. *Proc. Intl. Soc. Mag Reson. Med.* 19, 2019.
- Tournier, J. D., Yeh, C. H., Calamante, F., Cho, K. H., Connelly, A., and Lin, C. P. (2008). Resolving crossing fibres using constrained spherical deconvolution: validation using diffusion-weighted imaging phantom data. *Neuroimage* 42, 617–625. doi: 10.1016/j.neuroimage.2008.05.002
- Verstynen, T., Jarbo, K., Pathak, S., and Schneider, W. (2011). *In vivo* mapping of microstructural somatotopies in the human corticospinal pathways. *J. Neurophysiol.* 105, 336–346. doi: 10.1152/jn.00698.2010
- Volkman, J., Herzog, J., Kopper, F., and Deuschl, G. (2002). Introduction to the programming of deep brain stimulators. *Mov. Disord.* 17, S181–S187. doi: 10.1002/mds.10162
- von Monakow, K. H., Akert, K., and Künzle, H. (1979). Projections of precentral and premotor cortex to the red nucleus and other midbrain areas in Macaca fascicularis. *Exp. Brain Res.* 34, 91–105. doi: 10.1007/BF00238343
- Voorn, P., Vanderschuren, L. J., Groenewegen, H. J., Robbins, T. W., and Pennartz, C. M. (2004). Putting a spin on the dorsal-ventral divide of the striatum. *Trends Neurosci.* 27, 468–474. doi: 10.1016/j.tins.2004.06.006
- Weinberger, D. R. (1987). Implications of the normal brain development for the pathogenesis of schizophrenia. *Arch. Gen. Psychiatry* 44, 660–669. doi: 10.1001/archpsyc.1987.01800190080012
- Wise, R. A. (2009). Roles for nigrostriatal—not just mesocorticolimbic—dopamine in reward and addiction. *Trends Neurosci.* 32, 517–524. doi: 10.1016/j.tins.2009.06.004
- Wu, Y. R., Levy, R., Ashby, P., Tasker, R. R., and Dostrovsky, J. O. (2001). Does stimulation of the GPI control dyskinesia by activating inhibitory axons? *Mov. Disord.* 16, 208–216. doi: 10.1002/mds.1046
- Zakiewicz, I. M., Bjaalie, J. G., and Leergaard, T. B. (2014). Brain-wide map of efferent projections from rat barrel cortex. *Front. Neuroinform.* 8:5. doi: 10.3389/fninf.2014.00005
- Zhang, H. Y., Tang, H., Chen, W. X., Ji, G. J., Ye, J., Wang, N., et al. (2015). Mapping the functional connectivity of the substantia nigra, red nucleus and dentate nucleus: a network analysis hypothesis associated with the extrapyramidal system. *Neurosci. Lett.* 606, 36–41. doi: 10.1016/j.neulet.2015.08.029
- Zhou, F. M., and Lee, C. R. (2011). Intrinsic and integrative properties of substantia nigra pars reticulata neurons. *Neuroscience* 198, 69–94. doi: 10.1016/j.neuroscience.2011.07.061

Conflict of Interest Statement: The authors declare that the research was conducted in the absence of any commercial or financial relationships that could be construed as a potential conflict of interest.

Copyright © 2016 Cacciola, Milardi, Anastasi, Basile, Ciolli, Irrera, Cutroneo, Bruschetta, Rizzo, Mondello, Bramanti and Quartarone. This is an open-access article distributed under the terms of the Creative Commons Attribution License (CC BY). The use, distribution or reproduction in other forums is permitted, provided the original author(s) or licensor are credited and that the original publication in this journal is cited, in accordance with accepted academic practice. No use, distribution or reproduction is permitted which does not comply with these terms.